CENTENNIAL FEATURE ARTICLE

Rate Constant Rules for the Automated Generation of Gas-Phase Reaction Mechanisms†

Hans-Heinrich Carstensen and Anthony M. Dean*

Chemical Engineering Department, Colorado School of Mines, Golden, Colorado 80401

Received: June 4, 2008; Revised Manuscript Received: September 30, 2008

The capability of kinetic models to predict complex chemical systems has enormously improved in the last decades, making them an increasingly important tool for process development and optimization. Extension of these approaches to even more complex systems is hindered not only by the geometrically increasing number of reactions and species to be considered but also by the necessity of assigning accurate rate constants to all of the reactions. The recent developments in automated mechanism generators can address the tedious bookkeeping issues. The requirement for development of accurate rate constant estimates remains the job of the kineticist. This task has been aided immeasurably by the combined advances in electronic structure methods and computer performance. This article describes two areas of rate estimation. First, we discuss the development of H abstraction rate estimates from C−H bonds in alkanes, cycloalkanes, and allylic systems by H atoms and point to a surprising result found for cyclopentane. Second, we briefly review our investigation of the ethyl + O_2 reaction and demonstrate the suitability of the QRRK/MSC approach for automated mechanism generation. We conclude with some suggestions for future work in this area.

Introduction

Since its beginnings some 50 years ago, detailed chemical kinetic modeling of gas-phase reaction systems has progressed enormously, and today it is established as a powerful tool. It is now routinely applied to a broad range of areas including atmospheric chemistry and air pollution,[1,2] ignition time[3] and exhaust modeling in internal combustion engines,[4] emission control in waste incineration,[5] feed gas conversion in solid oxide fuel cells,[6,7] thermal conversion of biomass,[8] and many others.

A part of the reason for the success of kinetic models is increasing computing power, which enables modelers to use more and more complex kinetic and reactor models and to generate predictions in an acceptable time. Besides improvements in the hardware (faster CPUs, increases in memory and storage capacity, parallelization in supercomputers), significantly more efficient algorithms are now available to solve the stiff ODEs of the underlying energy, transport, and mass interaction equations. Further, program packages such as Chemkin,[9] Cantera,[10] or Detchem[11] allow even rather inexperienced users to set up a reactor model and to define the chemistry. New strategies, for example, the concept of adaptive chemistry,[12,13] divide a reacting system into different zones and use only as much chemistry as needed to solve highly demanding coupled kinetic-transport problems. Analytic software, which can be integral parts of the kinetic solvers or external add-ons such as KinalC,[14] provides valuable rate and sensitivity analysis information, which helps to improve mechanistic predictions or can be used as input for mechanism reduction algorithms. Smaller but still accurate reaction sets again speed up the calculations and expands the range of applicability of detailed chemistry.

Although numerical packages play an essential role in the modeling process, the most important key for success is the chemistry information used. The inherent complexities of technical applications and the ever increasing demands for higher accuracy and reliability of the simulations have already led to mechanisms that contain hundreds of species and thousands of reactions; the size of future reaction sets will probably grow even more. In the past, such mechanisms (including thermodynamic data and reaction sets) have been compiled manually, and the model developer depended almost entirely on experimental results to assign reaction pathways and rate coefficients. Whenever available, thermodynamic and kinetic data from carefully designed measurements (e.g., refs 15−18) are (and will probably remain) the preferred source of input. However, compared to the volume of input data needed, the amount of available experimental information is scarce. Further, these data are often only valid for a narrow range of conditions that might be far removed from those of the application. In recent years, high-level electronic structure calculations have matured to a point that they reach a level of precision almost comparable to well-defined experimental measurements. Combined with statistical mechanics, transition-state theory, and RRKM and/or QRRK theory, these calculations provide now a complementary source for the required input parameters. However, even though those calculations are significantly faster than measurements, they still cannot provide the amount of input that will be needed to generate the large mechanisms of the future. Not only is the number of reactions so large that it is not possible to compute all of the required info, but also the number of atoms in species can become too

† 2008 marked the Centennial of the American Chemical Society's Division of Physical Chemistry. To celebrate and to highlight the field of physical chemistry from both historical and future perspectives, *The Journal of Physical Chemistry* is publishing a special series of Centennial Feature Articles. These articles are invited contributions from current and former officers and members of the Physical Chemistry Division Executive Committee and from *J. Phys. Chem.* Senior Editors.

* To whom correspondence should be addressed.

10.1021/jp804939v CCC: $40.75
Published on Web 12/17/2008

Hans-Heinrich Carstensen is a research associate professor in the Chemical Engineering Department at Colorado School of Mines (CSM). He received his Ph.D. in chemistry from the university in Goettingen, Germany. After several post doctorial appointments at the Sandia Livermore National Lab (1995-1996), Exxon Research and Engineering (1996-1999), and Massachusetts Institute of Technology (1999-2000), he joined the research group of Prof. A. Dean at CSM in 2000. His main research interests are in using electronic structure calculations to develop elementary pressure-dependent reaction mechanisms for combustion, biomass conversion, and fuel cell technology.

Anthony M. Dean is the W. K. Coors Distinguished Professor in the Chemical Engineering Department at the Colorado School of Mines. He received his B.S. in chemistry from Spring Hill College and his Ph.D. in physical chemistry from Harvard University. He joined the Chemistry Department of the University of Missouri—Columbia in 1970, where his research program involved shock tube studies of elementary combustion-related reactions. In 1979, he moved to the Corporate Research Labs of Exxon Research and Engineering and focused on the quantitative kinetic characterization of gas-phase combustion systems. He joined the CSM faculty in 2000, where his group currently studies the kinetics within solid-oxide fuel cells and the kinetics of biomass pyrolysis and gasification.

big to perform such calculations at a level high enough to obtain reliable information. One solution to this dilemma is to use high-quality calculations of model systems as the basis for the creation of "rules" that can then be applied to a range of analogous reactions.

The manual creation of gas-phase reaction mechanisms is not only a tedious and time-consuming procedure, but it is also prone to errors and incompleteness in the reaction network and species pool. Essentially, the generation process involves two steps, (1) the identification of all necessary species and all important reactions within the pool of reactants and (2) the assignment of thermodynamic data for the species and rate expressions for the reactions. Both steps are closely coupled since the decision of which species and reactions to keep is only possible if equilibrium constants and rate expressions are known. Within the last 15 years or so, algorithms have been developed that perform these steps fully automatically.[19−30] Chemical species and reactions are formulated in terms of matrices and operations that allow the use of a computer to systematically create the full set of theoretically possible reactions. Of course, this leads to an enormously large number of reactions for which rate constants have to be assigned. Again, experimental or theoretical databases are easily exhausted, and automated mechanism generators depend even more heavily on estimation methods than manually created ones. Group additivity[31−33] has proven to be a reliable and accurate approach to estimate thermodynamic properties for stable molecules and radicals. Therefore, it appears that the major remaining obstacle for the generation of accurate kinetic computer-generated models is the availability and accuracy of rate estimation methods. The role of the kineticist—now relieved from the cumbersome bookkeeping job of actually generating reaction mechanisms—is then to define adequate reaction classes and to develop appropriate rate estimation rules for these.

Attempts to generalize the reactivity of chemicals have been made for many years, and a review by Sumathi et al.[34] has addressed their applicability toward kinetic modeling. The most widely used rate rules are related to the so-called linear free energy relationship (LFER). We can understand the basic idea by examining the transition-state theory (TST) equation of a rate constant in terms of the Gibbs free energy

$$k(T) = \kappa(T) \cdot k_B T/h \cdot V_m^{(n-1)} \cdot \exp(-\Delta G^{\#}/RT)$$

Here, $\kappa(T)$ is the tunneling correction factor, V_m the molar volume for standard condition, n the molarity of the reaction (e.g., $n = 1$ for unimolecular, $n = 2$ for bimolecular), and $\Delta G^{\#}$ the difference in free energy between the transition-state geometry and the reactant(s) minus the contribution from the reaction path mode, and the remaining symbols represent common physical constants or variables. If tunneling can be ignored or assumed constant for a set of reactions, the LFER is obtained

$$\ln(k(T)) = \ln(k^{\mathrm{ref}}(T)) - 1/RT \cdot (\Delta G^{\#} - \Delta G^{\#,\mathrm{ref}})$$

Within a reaction family, the $\Delta S^{\#}$ term remains approximately constant, hence

$$\ln(k(T)) = \ln(k^{\mathrm{ref}}(T)) - 1/RT \cdot (\Delta H^{\#} - \Delta H^{\#,\mathrm{ref}})$$

which relates differences in the logarithmic rate constants of a reaction family to changes in the barrier heights. An application of this is the well-known Hammett equation

$$\ln(k(T)) = \ln(k^{\mathrm{ref}}(T)) + \rho\sigma$$

in which the Hammett σ parameter[35] is a measure of the impact a substituent has on the reaction rate constant and ρ is a reaction class specific constant. Hammett and later Taft[36] identified resonance, induction, hyperconjugation, and steric effects as stabilizing or destabilizing factors for transition states.

Another widely used relationship is attributed to Evans and Polanyi.[37,38] It is based on the observation that changes in the reaction exothermicity translate linearly into changes of the barrier height

$$\Delta H^{\#} = E_a + m \cdot \Delta_R H$$

This leads to

$$E_a = E_a^{\mathrm{ref}} + m(\Delta_R H - \Delta_R H^{\mathrm{ref}}) = \mathrm{constant} + m \cdot \Delta_R H$$

More recently developed rate estimation approaches take advantages of the improvements in electronic structure methods since these calculations allow separately the investigation of pre-exponential factors and barriers. One approach extends Benson's group additivity method to transition states.[39−41] For each different reactive center, a new "supergroup" (contains more than one polyvalent atom) with its own set of enthalpy, entropy, and heat capacity values is created. Since the supergroups for H abstraction reactions from, for example, oxygenates or allylic C−H bonds are different from those of regular alkanes, this approach naturally leads to a very detailed classification of reaction classes. Another advantage of this approach is that steric effects can easily be incorporated via non-next-neighbor groups.

A conceptually similar but differently implemented method is employed by Zhang et al.[42] The so-called extended reaction

class transition-state theory (RC-TST/LER) method uses an Evans−Polanyi relationship to estimate reaction barriers and determines the pre-exponential factor (relative to a well-characterized reference reaction) by performing a cost-effective molecular mechanics or DFT calculation with statistical analysis. A characteristic of this approach is that the various contributions (different internal modes, symmetry, tunneling) to the partition functions are separately analyzed and generalized. By doing so, the analysis shows which contributing factor has the largest impact on variations of a rate constant within a reaction class.

In our approach, we develop rate estimation rules that are simpler than both previously described methods. The temperature dependence of rate expressions of a reaction family is expressed in terms of a fixed temperature exponent n and a barrier E that is related to the exothermicity of a reaction (Evans−Polanyi relationship). The pre-exponential factor is determined from a reference reaction or by averaging rate constants of a test set of reactants. For hydrogen abstraction reactions, the pre-exponential term is expressed on a per bond type basis and is assumed to scale with the number of hydrogens of that particular bond type. This type of rate estimation method has been used for many years, but in the past its use was limited by a lack of comprehensive sets of available rate expressions. Now, we are in the position to explore its feasibility by using a wide range of theoretically derived kinetic data. One concern related to this approach is the scope or range for which a single rate rule may be applied. How similar must a reaction be to the reference reaction to ensure that an estimated rate constant is still a good approximation of its "true" value? This directly points to a related issue, which is how many separate reactions classes (and thus rules) are required to predict the rate coefficients. We will discuss some of these issues in greater detail using the H abstraction reaction by H atoms from aliphatic alkanes, cycloalkanes, and allylic C−H bonds as examples.

The rate estimation techniques discussed above provide high-pressure rate expressions, which can be used "as is" for abstraction reactions. All other reaction types are, at least under certain conditions, pressure-dependent. State-of-the-art methods[43−45] to calculate pressure-dependent rate constants require detailed molecular parameters of the species and transition states involved; hence, they are not feasible for automated mechanism generators. The simpler QRRK approach[46] on the other hand relies on the same estimation methods as those used for pressure-independent reactions. We will review aspects of the QRRK analysis of the reaction of ethyl with molecular oxygen to demonstrate that this approach is simple but accurate at the same time.

A discussion of future directions in this area concludes this article.

Calculation Methods

With the development of composite methods, electronic structure calculations became capable of predicting thermodynamic properties to "chemical accuracy", which is normally defined as to within 1−2 kcal/mol of experimental data. Given the exponential dependence, this level of uncertainty in the enthalpy or barrier height contributes significantly less error at elevated temperatures than at low temperatures. The latest versions of composite methods such as the G3 method by Curtiss[47] and co-workers and the CBS-QB3 method by Petersson et al.[48] achieve average accuracies of just over 1 kcal/mol when compared to a large test set of well-established experimental values. Both methods can be applied to species containing up to about 10 heavy (non-hydrogen) atoms on moderately equipped work stations. Even higher accuracy can be achieved with CBS-APNO[49] or other benchmark methods, such as the Wn series by Martin[50] or coupled cluster methods with large basis sets and extrapolation to the CBS limit,[51] however at the expense that they can only be applied to small molecules.

While the performance of these methods has been well assessed for stable molecules, much less is known about their accuracy when it comes to reaction barriers and rate constants. Recently, Vandeputte et al.[52] investigated the ability of CBS-QB3, G3B3,[47] and two DFT methods (MPW1PW91/6-311G(2d,d,p)[53] and BMK/6-311G(2d,d,p))[54] to predict rate constants for 21 H abstraction reactions by methyl radicals. The conclusion was that the CBS-QB3 method performs best. In agreement with this, previous studies on H abstraction reactions by HO_2 and alkyl peroxy radicals[55] in our group also found that this method yields rate constants in good agreement with the available experimental data. Therefore, the CBS-QB3 method was used for the calculations presented in this paper.

All calculations were performed with the G98W[56] and G03[57] suites of programs. The CBS-QB3 composite method optimizes the molecule's geometry at the B3LYP/6-311G(2d,d,p)[58] level. On the basis of this geometry, frequency and higher level energy calculations at the CCSD(T)/6-31+G(d′) and MP4(SDQ)/6-31G+(d,p) levels are performed to obtain the final energy which includes spin−orbit corrections.

The molecular parameters of reactants, products and transition states from the CBS-QB3 calculations serve as input for a standard statistical mechanics treatment to calculate thermodynamic properties of the species. The atomization method is used to convert the electronic energy of a species into a corresponding heat of formation. Since this work focuses on rate expressions, only relative energies are needed, and no attempts were made to improve on absolute heat of formation values, for example, by applying bond additivity corrections. Except for internal modes resembling (hindered) internal rotations, we assume that the harmonic oscillator rigid rotor approximation holds. The harmonic frequencies are scaled by a factor of 0.99. Contributions from internal rotations are incorporated in the following way. First, we calculate for each single bond the hindrance potential at the B3LYP/6-31G(d) level of theory via a relaxed potential energy scan in steps of 20° (or less) of the dihedral angle around the bond. We then inspect this potential for (a) minima that are lower than the starting geometry to identify the lowest energy conformer at 0 K, which is used throughout this work, and (b) for the total barrier height. If the hindrance potential is sufficiently low (a threshold of <10 kcal/mol is arbitrarily chosen), we replace the corresponding frequency, which is identified visually from its animation, with a hindered rotor partition function and leave all other frequencies unchanged. This potential is then approximated with a truncated Fourier series ($n = 5$). The corresponding averaged moments of inertia for the rotation are determined at the $I^{(2,3)}$ level as defined by East and Radom[59] based on the work by Kilpatrick and Pitzer.[60] With this information at hand, the Schroedinger equation can be solved numerically using the wave functions of the free rotor as basis functions. The solution is a set of energy eigenvalues, which are used to calculate the contribution of this mode to the thermodynamic functions H, S, and C_p.

All reported rate constants have been calculated with canonical transition-state theory (cTST), formulated in terms of the Gibbs free energy (see above). The temperature-dependent transmission factor $\kappa(T)$, which accounts for contributions from tunnelling, is obtained from asymmetric Eckart potentials.[61] The correction factors obtained in this way differ in most cases only marginally from previous calculations in which we used the

TABLE 1: H Abstraction by H Atoms from CH_4 and Primary C−H Groups in Linear and Branched Alkanes[a]

		mod. Arrh. parameters			$k_{rate\ rule}/k_{TST}$		
reaction	n_H	A_H	n	E	500 K	1000 K	1500 K
$CH_4 \rightleftharpoons CH_3$	4	7.50E6	2.07	11.2	–	–	–
			Primary C−H				
$C_2H_6 \rightleftharpoons C_2H_5$	6	1.79E7	1.95	8.17	0.87	0.90	0.91
		1.49E7	**1.97**	**8.13**			
CCC ⇌ CCC•	6	1.68E7	1.96	8.13	0.85	0.89	0.90
		1.49E7	**1.97**	**8.10**			
CCCC ⇌ CCCC•	6	1.82E7	1.94	8.30	1.02	0.99	0.98
		1.44E7	**1.97**	**8.25**			
CCCCC ⇌ CCCCC•	6	1.76E7	1.94	8.27	1.04	1.03	1.03
		1.35E7	**1.97**	**8.21**			
CCCCCC ⇌ CCCCCC•	6	1.75E7	1.94	8.31	1.06	1.02	1.02
		1.39E7	**1.97**	**8.26**			
CCC2 ⇌ C2CC•	9	1.43E7	1.97	8.35	1.14	1.06	1.04
		1.41E7	**1.97**	**8.34**			
CCCC2 ⇌ C2CCC•	3	1.06E7	1.99	8.14	1.10	1.12	1.12
		1.23E7	**1.97**	**8.17**			
CCCCC2 ⇌ C2CCCC•	3	2.14E7	1.93	8.21	0.83	0.84	0.85
		1.60E7	**1.97**	**8.15**			
CCCC2 ⇌ CCCC2•	6	1.46E7	1.95	8.29	1.20	1.16	1.16
		1.23E7	**1.97**	**8.26**			
CCCCC2 ⇌ CCCCC2•	6	1.48E7	1.96	8.23	1.06	1.06	1.05
		1.32E7	**1.97**	**8.21**			
CCC3 ⇌ C3CC•	12	1.35E7	1.98	8.39	1.22	1.11	1.07
		1.40E7	**1.97**	**8.40**			
CCCC3 ⇌ C3CCC•	3	6.45E6	2.05	8.07	1.15	1.17	1.16
		1.20E7	**1.97**	**8.19**			
CCCC3 ⇌ CCCC3•	9	9.29E6	2.01	8.30	1.26	1.17	1.13
		1.30E7	**1.97**	**8.36**			
CCC(C)CC ⇌ CCC(C)CC•	6	1.01E7	2.01	8.03	0.91	0.96	0.97
		1.37E7	**1.97**	**8.09**			
CCC(C)CC ⇌ CCC(C•)CC	3	1.13E7	2.00	8.13	0.96	0.97	0.97
		1.42E7	**1.97**	**8.18**			
average (restricted fits)		**1.4E7**	**1.97**	**8.2**			
standard deviation		**1.1E6**		**0.1**			

[a] The reactions are abbreviated (reactant H and product H_2 omitted) to improve readability. The units are cm^3/mol-s and kcal/mol, respectively. The rate constant $k_{rate\ rule}$ has been calculated using the average values listed at the bottom of the table. The rows in bold type list refitted parameters with the n values fixed at the average value. The ratio uses the original k_{TST} value. Molecule structures are presented in abbreviated form (H atoms missing, radical site marked with "•"), for example, CCC3 represents neopentane, to improve readability.

simpler correction formula by Wigner;[62] however, the differences increase for reactions with small barriers. In those cases, Eckart tunneling corrections or more sophisticated methods such as the small-curvature tunneling approach[63] are needed to obtain reliable rate expressions at low temperatures. According to Truong et al.,[64] the small-curvature tunneling method yields at 300 K about a factor of 2−4 higher than the Eckart method for H abstraction reactions from fluorine-substituted methanes. Since uncertainties in barrier heights lead to a similar degree of uncertainty (Figure 1) and small-curvature tunneling corrections require a substantial amount of additional calculations, we decided to restrict ourselves to the use of Eckart correction factors. Rate constants calculated for the temperature range of 300−2500 K in steps of 50 K were approximated with the modified Arrhenius expression. The maximum errors in these fits were typically on the order of 10% or less.

Rate Constant Estimations for H Abstraction from Alkanes, Cycloalkanes, and Allylic C−Hs in Alkenes by H Atoms. ***1. Alkanes.*** Since theoretically obtained rate estimation rules will be a central part of future mechanisms, it is important to access their accuracy and applicability range. We investigated this for H abstractions by H atoms in two steps. First, we calculated rate estimation rules for alkanes, which are applied, in the second step, to predict the reactivity of cycloalkanes. In addition, we compared those to rate rules for allylic C−H bond abstractions. Rate expressions for H abstractions were calculated from the following sites: CH_4, R−CH_3, R−CH_2−R′, and RR′R″CH, with R, R′, R″ representing linear or branched alkyl chains. The reaction set is listed in Table 1 for CH_4 and CH_3 groups, in Table 2 for CH_2 moieties, and in Table 3 for CH sites. The calculated rate constants are reported in the form

$$k(T) = n_H \cdot A_H \cdot T^n \cdot \exp(-E/RT)$$

Here, n_H is the number of equivalent hydrogen atoms, A_H is the pre-exponential factor per H, n is the temperature coefficient (exponent), and E is a parameter related to the activation energy in the original Arrhenius expression. Even though it is not technically the activation energy (differing by nRT), we will refer to it as such in the remainder of the text.

The modified Arrhenius parameters have been obtained by least-squares minimization to $k(T)$ data from 300 to 2500 K in steps of 50 K. For each reaction except that with methane, two sets of modified Arrhenius parameters are given. Focusing on the rate expressions for H abstraction for primary C−H groups in Table 1, the upper set of rate constants for each reaction is obtained from fits in which all three parameters (A_H, n, E) are independently optimized. Inspection of the results for the entire set of reactions shows that these parameters fluctuate around some average values. The same can be seen for the other two

TABLE 2: H Abstraction by H Atoms from Secondary C−H Groups in Linear and Branched Alkanes (see Table 1 for explanatory notes)

		mod. Arrh. parameters			k_{rule}/k_{TST}		
reaction	n_H	A_H	n	E	500 K	1000 K	1500 K
CCC ⇒ CC•C	2	5.24E7	1.82	5.78	1.09	1.02	1.00
		4.32E7	**1.86**	**5.73**			
CCCC ⇒ CCC•C	4	5.27E7	1.82	5.71	1.04	1.01	1.00
		3.94E7	**1.86**	**5.65**			
CCCCC ⇒ CCCC•C	4	4.17E7	1.85	5.63	1.00	0.99	0.99
		3.95E7	**1.86**	**5.62**			
CCCCC ⇒ CCC•CC	2	4.48E7	1.83	5.56	0.95	0.99	1.01
		3.74E7	**1.86**	**5.52**			
CCCCCC ⇒ CCCCC•C	4	4.57E7	1.84	5.66	0.98	0.96	0.96
		4.11E7	**1.86**	**5.64**			
CCCCCC ⇒ CCCC•CC	4	3.46E7	1.86	5.49	0.96	1.01	1.03
		3.65E7	**1.86**	**5.50**			
CCCC2 ⇒ C2CC•C	2	2.78E7	1.88	5.58	1.22	1.22	1.22
		3.21E7	**1.86**	**5.61**			
CCCCC2 ⇒ C2CCC•C	2	3.03E7	1.91	5.85	1.16	0.99	0.93
		4.72E7	**1.86**	**5.94**			
CCCCC2 ⇒ C2CC•CC	2	3.63E7	1.85	5.59	1.10	1.11	1.11
		3.47E7	**1.86**	**5.58**			
CCCC3 ⇒ C3CC•C	2	3.19E7	1.87	5.48	1.02	1.08	1.10
		3.43E7	**1.86**	**5.50**			
CCC(C)CC ⇒ CCC(C)C•C	4	2.39E7	1.89	5.67	1.46	1.38	1.35
		3.00E7	**1.86**	**5.72**			
average (restricted fits)		**3.8E7**	**1.86**	**5.6**			
standard deviation		**5.0E6**		**0.13**			

TABLE 3: H Abstraction by H Atoms from Tertiary C−H Groups in Branched Alkanes (see Table 1 for explanatory notes)

		mod. Arrh. parameters			k_{rule}/k_{TST}		
reaction	n_H	A_H	n	E	500 K	1000 K	1500 K
CCC2 ⇒ CC•C2	1	1.24E8	1.72	3.84	1.04	0.99	0.98
		9.57E7	**1.75**	**3.79**			
CCCC2 ⇒ CCC•C2	1	1.06E8	1.71	3.74	1.15	1.16	1.17
		7.73E7	**1.75**	**3.68**			
CCCCC2 ⇒ CCCC•C2	1	9.15E7	1.75	3.69	0.97	0.97	0.97
		9.33E7	**1.75**	**3.69**			
C2CCC2 ⇒ C2CC•C2	2	5.10E7	1.84	3.55	0.90	0.92	0.91
		1.00E8	**1.75**	**3.68**			
CCC(C)CC ⇒ CCC•(C)CC	1	1.02E8	1.73	3.68	0.96	0.99	1.00
		8.98E7	**1.75**	**3.65**			
average (restricted fits)		**9.1E7**	**1.75**	**3.7**			
standard deviation		**2.8E6**		**0.05**			

reaction families (secondary and tertiary C−H). Simply taking averages would not lead to a good generic rate expression because these parameters are strongly coupled. Instead, we average only the n values, which are relatively constant. With these average n values determined and kept constant at 1.97, 1.86, and 1.75 for primary, secondary and tertiary C−H abstractions, respectively, reoptimization of A_H and E_a leads to the alternative sets of Arrhenius values that are presented in bold below the original values. The new A_H and E_a values show clearly less variations than the original parameters, hence providing better rate rules. Taking into account that the accuracy is certainly not better than two digits, we arrive at the recommended generic rate rules

prim. C−H:

$$k = n_H \cdot 1.4E7\ \mathrm{cm^3/mol\text{-}s} \cdot T^{1.97} \cdot \exp(-8.2\,\mathrm{kcal\,mol^{-1}}/RT)$$

sec. C−H:

$$k = n_H \cdot 3.8E7\ \mathrm{cm^3/mol\text{-}s} \cdot T^{1.86} \cdot \exp(-5.6\,\mathrm{kcal\,mol^{-1}}/RT)$$

tert C−H:

$$k = n_H \cdot 9.1E7\ \mathrm{cm^3/mol\text{-}s} \cdot T^{1.75} \cdot \exp(-3.7\,\mathrm{kcal\,mol^{-1}}/RT)$$

In order to demonstrate the quality of these rate estimation rules, we calculated rate constants using these rules for all reactions at 500, 1000, and 1500 K and report in Tables 1−3 the ratios of the rule-based values to individually TST-calculated rate constants. With a few exceptions, we find that the estimated rate constants are at all temperatures within 20−25% of the TST rate constants, and in many cases, the agreement is better than 10%. The worst agreement for primary C−H abstraction is obtained for neo-hexane ($CCCC_3$) leading to the formation of the $CCCC_3$• radical at 500 K, where the deviation is 26%. A possible explanation for the observed deviation could be that our electronic structure calculations do not sufficiently capture the steric interactions of the crowded $(CH_3)_3C$ moiety, which may lead to inaccurate energies and/or numerical frequencies. Small changes in low-frequency values have a large impact on the entropy term and consequently on the A factors in rate constants. The fact that the results obtained for branched alkanes fluctuate more than those for linear alkanes seems to support this idea. Of course, another possibility is the existence of small

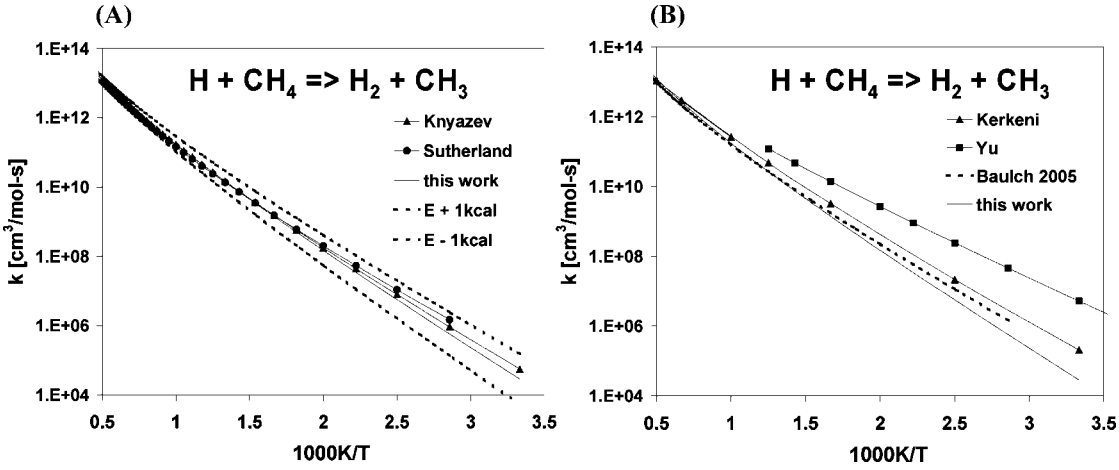

Figure 1. Rate constant comparison for H + CH_4 ⇒ H_2 + CH_3 (see text for details).

"real" steric non-next-neighbor interactions, but our results do not show any systematic trend that would support this. In the secondary C−H bonds reaction set (Table 2), we notice that the rate constant for the reaction H + CCC(C)CC leading to CCC(C)C•C is an outlier. The deviation of the rate rule from its TST rate constant is almost 50% at 500 K, clearly outside of the range of deviations seen for all other reactions. We were not able to identify an obvious problem in the calculations of this reaction and cannot provide, at this time, an explanation for this deviation. Looking at the data for tertiary C−H abstraction in Table 3, the results are remarkably consistent and seem to contradict our suspicion that sterically demanding molecules might lead to less "reliable" calculation results.

Although these results indicate that the TST results can be generalized into simple rate rules, it is necessary to compare these results to reliable literature data to confirm their accuracy. To do so, we compare the rate expression for H abstraction from CH_4 with experimentally derived rate constants (Figure 1 left) and with rate constants from theoretical predictions or extensive reviews (Figure 1 right). Sutherland et al.[65] performed laser photolysis/shock tube experiments to obtain the rate constants for 928−1697 K. H atoms were detected via atomic resonance absorption. The authors also used TST calculations based on a PES by Kraka et al.[66] to essentially reproduce the experimental data and to extend the range down to 300 K. Bryukov and co-workers[67] report discharge flow/resonance fluorescence measurements between 748 and 1054 K and show that their results agree well with older experimental observations. Figure 1 shows that the present calculated results are very close to the experimental data and that adjustments of the barrier by less than 1 kcal/mol would lead to almost perfect agreement. Among the many theoretical studies of this reaction, only a few recent ones can be mentioned here. Quantum scattering calculations by Kerkeni et al.[68] yield rate constants that are, at low temperatures, consistently higher than the experimental values but approach those at higher temperatures. Very similar results (not shown in Figure 1 because they are almost indistinguishable from those of Kerkeni et al.) have been obtained by Huarte-Larranaga et al.[69] (dynamic calculations) and by Pu et al.,[70] who performed TST and various levels of vTST calculations. On the other hand, quantum scattering calculations by Yu et al.,[71] using the same analytical H + CH_4 PES[72] as the previous two mentioned studies, are in much better agreement with the recommendations by Baulch et al.[73] and our values.

In summary, our calculations predict a very reasonable rate constant for H abstraction from methane by H atoms, and

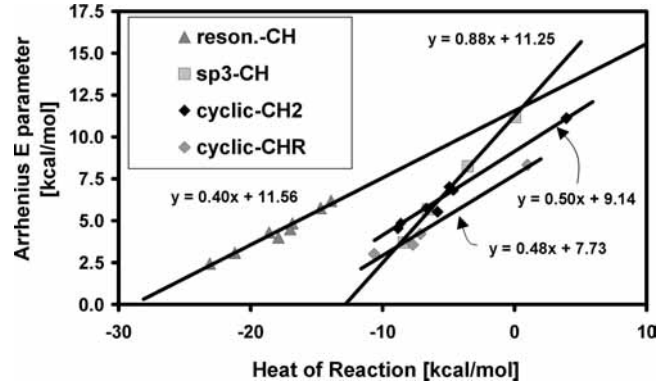

Figure 2. Evans−Polanyi plot for H abstraction reactions from various C−H bond types.

assuming that the uncertainty is similar for larger hydrocarbons, this provides confidence in the accuracy of the above-derived rate estimation rules. It should be noted that little reliable data is available for the reaction rate constants for higher alkanes, especially over a wide temperature range. For ethane, Tsang and Hampson[74] recommended the rate expression 5.54E2 cm^3/mol•s • $T^{3.5}$ • exp(−5.17 kcal/mol/*RT*), which has a much stronger Arrhenius curvature than our predicted temperature exponent. On the other hand, Baulch et al.[73] suggest for this reaction a rate constant with $n = 0$ (no curvature on an Arrhenius plot), $k(T)$ = 9.82E13 cm^3/mol•s • exp(−9.22 kcal/mol/*RT*). Realizing the ambiguity in the rate constant for ethane, we did not attempt to compare our rate constants for higher alkanes to other data.

A plot of the barrier height against the heat of reaction reveals an approximately linear relationship (see Figure 2), as has been observed before.[39,42] The slope is approximately 0.88, which is considerably higher than the slope of 0.65 derived from the evaluation of the sparse set of experimental data.[75] The lowering of the transition-state energy closely follows the reaction exothermicity. Since the radicals are stabilized via hyperconjugation, one could interpret this finding in the way that almost 90% of the hyperconjugative stabilization experienced by alkyl radicals gets translated to the corresponding transition state, leading to a significantly lower activation energy as the level of hyperconjugative stability is increased.

2. Cycloalkanes. Having generic rate constants for CH_2 and CH moieties in noncyclic alkanes in hand, one might expect that these rules could also provide good estimates for moderately sized cycloalkanes. To test this hypothesis, we conducted

TABLE 4: Reaction Rate Constants for Abstraction from CH_2 Groups in Cycloalkanes and Comparison between TST Rate Constants and the Rate Estimation Rule for Secondary C−H Bonds in Noncyclic Alkanes (see Table 1 for explanatory notes)[a]

reaction	n_H	mod. Arrh. parameters A_H	n	E	$\Delta_R H^{298}$	$k_{est.}/k_{TST}$ 1000 K	$k_{est.}/k_{TST}$ 1500 K
rate rule for sec.CH_2		**3.80E7**	**1.86**	**5.6**	**−6.6**		
Unsubstituted Cycloalkanes							
CyC3 ⇒ cy(C•CC)	6	1.92E7	1.99	11.1	3.9	13.0	4.87
CyC4 ⇒ cy(C•CCC)	8	1.70E7	2.04	7.0	−5.0	1.28	0.95
CyC5 ⇒ cy(C•CCCC)	10	1.76E6	2.00	4.6	−8.9	5.02	5.66
CyC6 ⇒ cy(C•CCCCC)	12	1.30E7	1.99	5.5	−5.8	1.12	1.07
Methyl-Substituted Cycloalkanes							
CcyC3 ⇒ Ccy(CC•C)_sTS	2	1.96E7	1.98	11.4	3.9	15.6	5.67
CcyC3 ⇒ Ccy(CC•C)_aTS	2	2.87E7	1.95	11.0	3.9	10.8	4.23
CcyC4 ⇒Ccy(CC•CC)_sTS	2	1.12E7	2.01	6.7	−4.4	2.10	1.64
CcyC4 ⇒ Ccy(CC•CC)_aTS	2	1.63E7	2.02	6.9	−4.4	1.53	1.16
CcyC4 ⇒ Ccy(CCC•C)_sTS	1	1.32E7	2.04	6.9	−4.7	1.57	1.18
CcyC4 ⇒ Ccy(CCC•C)_aTS	1	1.06E7	2.04	6.4	−4.7	1.56	1.27
CcyC5 ⇒ Ccy(CC•CCC)_sTS	2	3.30E6	1.98	5.0	−8.4	3.66	3.88
CcyC5 ⇒ Ccy(CC•CCC)_aTs	2	4.96E6	1.98	5.3	−8.4	2.87	2.86
CcyC5 ⇒ Ccy(CCC•CC)_sTS	2	3.42E6	2.02	4.6	−8.8	2.29	2.54
CcyC5 ⇒ Ccy(CCC•CC)_aTS	2	3.57E6	2.00	4.6	−8.8	2.44	2.75
CcyC6 ⇒ Ccy(CC•CCCC)	4	1.33E7	1.98	5.6	−5.6	1.22	1.16
CcyC6 ⇒ Ccy(CCC•CCC)	4	1.35E7	2.00	5.5	−5.9	1.04	1.00
CcyC6 ⇒ Ccy(CCCC•CC)	2	1.45E7	2.00	6.0	−5.8	1.26	1.11

[a] sTS and _aTS indicate two different transition states; sTS marks abstraction from the same direction in which the CH_3 is oriented (syn), and aTS indicates abstraction anti to the CH_3 group.

TABLE 5: Reaction Rate Constants for Abstraction from R_2CH Groups in Cycloalkanes and Comparison between TST Rate Constants and the Rate Estimation Rule for Tertiary C−H Bonds in Noncyclic Alkanes (see Table 1 for explanatory notes)

reaction	n_H	mod. Arrh. parameters A_H	n	E	$\Delta_R H^{298}$	$k_{est.}/k_{TST}$ 1000 K	$k_{est.}/k_{TST}$ 1500 K
rate rule for tert.CH		**9.10E7**	**1.75**	**3.7**	**−8.40**		
Unsubstituted Cycloalkanes							
CcyC3 ⇒ Ccy(C•CC)	1	4.31E + 07	1.88	8.34	0.99	9.00	3.93
CyC4 ⇒ cy(C•CCC)	1	3.24E + 07	1.89	4.21	−7.14	1.35	1.17
CyC5 ⇒ cy(C•CCCC)	1	1.22E + 07	1.88	3.01	−10.64	2.23	2.38
CyC6 ⇒ cy(C•CCCCC)	1	3.41E + 07	1.87	3.57	−7.71	1.09	1.06

calculations for cycloalkanes containing three to six carbons and compared the TST rate constants with predictions using the rate rule for secondary C−H abstraction. The results are shown in Table 4, which also includes data for methyl monosubstituted cycloalkanes. The substituted species have CH_2 moieties with two different C−H sites, one where the bond in on the same side of the ring as the CH_3 group and one on the opposite side. Since at least theoretically these are not equivalent, we calculated individual rate constants for each C−H bonds. The results show little difference in the rate constants, indicating that, in practice, both C−H types can be considered equivalent.

The ratios between estimated and calculated rate constants at 1000 and 1500 K reveal that the rate rule for secondary CH_2 groups in noncyclic alkanes does not represent the reactivities of all cycloalkanes well. This is true for both unsubstituted and substituted cycloalkanes. The results show that the reactivities correlate well with ring size, meaning that $k_{estimated}/k_{TST}$ ratios for a given ring size are very comparable. H abstraction rate constants for cyclopropane and methyl cyclopropane are overpredicted by about an order of magnitude at 1000 K and roughly a factor of 5 at 1500 K. For C_4 rings, the overprediction is between 30% and a factor of 2.1 at 1000 K and, except for one case, within 30% for 1500 K. Interestingly, the deviations clearly increase for cyclopentane derivatives (up to a factor of >5 at both temperatures), while the rate constants for cyclohexane and its methyl derivative are well predicted.

Additional information provided in Table 4 points to several factors that lead to the failure of the noncyclic rate rule for cycloalkanes. First, the temperature exponent of the rate rule for noncyclic alkanes is clearly lower than the exponents found for all cycloalkanes. Among the cycloalkanes, these exponents are however remarkably constant. Second, the reaction exothermicity (the $\Delta_R H^{298}$ column in Table 4) varies dramatically with ring size and covers a range from 3.9 kcal/mol endothermic for C_3 rings to almost 9 kcal/mol exothermic for C_5 ring species. Finally, the pre-exponential factor (per hydrogen) for cyclopentane and its derivatives is significantly lower than the A factors for all other cycloalkanes.

To support these findings, we also looked at abstraction rate constants for tertiary C−H sites in cycloalkanes. These results are presented in Table 5 and confirm the observations made for CH_2 groups. Remarkably, even abstraction of a tertiary CH in cyclopropane by H atoms is slightly endothermic according to these CBS-QB3 calculations, while this reaction is about 2 kcal/mol more exothermic for methyl cyclopentane than that for noncyclic alkanes.

The possibly most surprising result is the trend in heats of reaction. A priori, one would expect that the C−H bond

TABLE 6: Reaction Rate Constants for Abstraction from Allylic CH_3 Groups in Alkenes and Comparison between TST Rate Constants and the Rate Estimation Rule for Primary C−H Bonds[a]

	mod. Arrh. parameters					$k_{rate\ rule}/k_{TST}$	
reaction	n_H	A_H	n	E_a	$\Delta_R H^{298}$ kcal/mol	1000 K	1500 K
CC=C ⇒ *C*=CC•	3	6.39E + 05	2.31	4.67	−18.2	1.24	1.15
		8.12E5	**2.28**	**4.72**			
trans-CC=CC ⇒ CC=CC•	6	8.10E + 05	2.28	4.32	−18.5	0.97	0.97
		8.43E5	**2.28**	**4.33**			
cis-CC=CC ⇒ CC=CC•	6	6.20E + 05	2.31	4.12	−19.7	0.96	0.98
		7.91E5	**2.28**	**4.17**			
trans-CCC=CC ⇒ CCC=CC•	3	8.39E + 05	2.28	4.37	−18.6	0.99	0.97
		8.55E5	**2.28**	**4.37**			
cis-CCC=CC ⇒ CCC=CC•	3	6.09E + 05	2.31	4.13	−19.22	0.97	0.98
		7.95E5	**2.28**	**4.19**			
trans-CCCC=CC ⇒ CCCC=CC•	3	8.82E + 05	2.28	4.34	−18.67	0.94	0.94
		8.71E5	**2.28**	**4.34**			
cis-CCCC=CC ⇒ CCCC=CC•	3	6.27E + 05	2.31	4.13	−19.25	0.94	0.96
		8.14E5	**2.28**	**4.18**			
C2C=C ⇒ *C*=CC2•	6	7.27E + 05	2.30	4.43	−16.96	1.05	1.02
		8.35E5	**2.28**	**4.45**			
CC=CC2 ⇒ C2C=CC•	3	8.43E + 05	2.27	3.84	−19.74	0.82	0.89
		7.76E5	**2.28**	**3.82**			
CC=CC2 ⇒ *c*-CC=CC2•	3	6.69E + 05	2.30	4.05	−18.10	0.91	0.94
		8.01E5	**2.28**	**4.08**			
CC=CC2 ⇒ *t*-CC=CC2•	3	8.26E + 05	2.28	4.09	−18.18	0.87	0.89
		8.46E5	**2.28**	**4.10**			
C2C=CC2 ⇒ C2C=CC2•	12	5.99E + 05	2.32	3.40	−19.87	0.64	0.73
		8.43E5	**2.28**	**3.47**			
CCC(C)=C ⇒ CCC(C•)=C*	3	1.18E + 06	2.13	3.04	−17.10	1.00	1.31
		7.46E5	**2.28**	**2.81**			
c-CC=CC=C ⇒ *C*=CC=CC•*	3	6.29E + 05	2.30	3.11	−25.70	0.61	0.74
		7.45E5	**2.28**	**3.15**			
t-CC=CC=C ⇒ C=CC=CC•	3	1.02E + 06	2.24	4.74	−24.40	1.28	1.20
		7.62E5	**2.28**	**4.68**			
C2C=CC=C ⇒ *c*-C=CC=CC2•	3	6.68E + 05	2.30	4.61	−24.30	1.25	1.18
		7.70E5	**2.28**	**4.64**			
C2C=CC=C ⇒ *t*-C=CC=CC2•	3	4.52E + 05	2.34	4.62	−22.49	1.36	1.26
		7.45E5	**2.28**	**4.72**			
C=C(C)C=C ⇒ C=C(C•)C=C*	3	1.56E + 06	2.22	6.00	−15.41	1.90	1.47
		9.39E5	**2.28**	**5.86**			
average (restricted fits)		**8.1E5**	**2.28**	**4.3**			
standard deviation		**3.8E4**		**0.35**			

[a] The reactions marked with *) are not used for averaging. See Table 1 for explanatory notes.

strengths in cyclopentane and cyclohexane are very similar and that both species should have similar heats of reaction. Experimental bond dissociation energies (BDEs) support this point of view (see, for example, ref 76). On the other hand, Tian et al.[77] report benchmark quality DBEs from electronic structure calculations (G3 and W1 level), which show that the bond strength in cyclopentane is 3−4 kcal/mol lower than those for cyclobutane and cyclohexane. This is in excellent agreement with the current study. The weak C−H bond appears to be an intrinsic property of (some) five-membered rings because we observe the same 3−4 kcal/mol BDE difference in methyl-substituted cycloalkanes. Special steric interactions in cyclopentane, the explanation offered by Tian et al. for its lower BDE compared to those of cyclobutane and cyclohexane, would also qualitatively explain why the *A* factor for its H abstraction reaction differs from those of other cycloalkanes. Our calculations did not reveal an obvious reason for the lower pre-exponential factor. However, the imaginary frequency of the transition state for cyclopentane (1091i) was about 40−50 cm^{-1} lower than those for cyclobutane (1134i) and cyclohexane (1149i). This is consistent with a smaller BDE in cyclopentane. Finally, it is worth pointing out that our kinetic analysis of the H abstraction reactions from cycloalkanes provides evidence that the discrepancy between the experimental and theoretical BDEs is probably not an artifact of the calculations because, as shown in Figure 2, the barrier for cyclopentane correlates well with those of the other cycloalkanes. Were erratic calculations at play, such a nice correlation would be unlikely.

3. Allylic C−H in Alkenes. H abstraction of an allylic H atom leads to a resonantly stabilized radical. Since resonance stabilization has been recognized for a long time as a reactivity-determining factor, we cannot expect the rate estimation rules for normal C−H groups to perform satisfactorily for allylic C−H. Indeed, application of the Evans−Polanyi relationship for sp^3 C−H in alkanes to H abstraction from allyl C−H bonds would predict a strongly negative and therefore unphysical barrier, indicating that this relationship cannot be used. In addition, we expect that the pre-exponential factors are smaller than those for regular C−H bonds because the alignment of the breaking bond to the neighboring double bond leads to a loss of entropy. These arguments suggest that separate estimation rules are needed for this reaction class. Table 6 presents our results for a series of abstraction reactions from allylic CH_3 groups. The entries

TABLE 7: H Abstraction by H Atoms from Allylic CH_2R and CHR_2 Groups in Alkenes (see Table 1 for explanatory notes)

reaction	n_H	mod. Arrh. parameters A_H	n	E_a	$k_{rate\ rule}/k_{TST}$ 500 K	1000 K	1500 K
Abstraction from Allylic CH_2R Groups							
CCC=C ⇒ CC=CC•	2	4.02E6	2.11	3.38	1.20	1.08	1.06
		2.49E6	**2.18**	**3.28**			
CCCC=C ⇒ CCC=CC• (2 diff. sites)	2	1.91E6	2.20	2.87	0.90	1.00	1.03
		1.86E6	**2.18**	**3.06**			
CCCC=C ⇒ CCC=CC• (2 diff. sites)	2	1.05E6	2.24	2.84	1.21	1.31	1.34
		1.79E6	**2.18**	**3.16**			
c-CCCC=CC ⇒ *c*-CCC=CC•C	2	1.13E6	2.89	2.27	0.99	1.03	1.03
		2.39E6	**2.18**	**3.04**			
t-CCCC=CC ⇒ *t*-CCC=CC•C	2	3.77E6	2.12	3.09	0.89	0.93	0.95
		2.55E6	**2.18**	**3.01**			
c-CCC=CC ⇒ *c*-CC=CC•C	2	1.70E6	2.23	3.02	0.95	0.95	0.95
		2.64E6	**2.18**	**3.11**			
t-CCC=CC ⇒ *t*-CC=CC•C	2	5.89E6	2.09	3.22	0.80	0.80	0.81
		3.06E6	**2.18**	**3.09**			
CCC(C)=C ⇒ C=C(C)C•C	2	3.56E6	2.13	3.07	0.89	0.93	0.96
		2.51E6	**2.18**	**3.00**			
C=CCC=C ⇒ *C*=CC=CC• (not used in rate rule)	2	1.87E7	1.84	2.58	0.64	1.05	1.32
		1.74E6	**2.18**	**2.05**			
average (restricted fits)		**2.4E7**	**2.18**	**3.1**			
standard deviation		**4.1E6**		**0.10**			
Abstraction from Allylic CHR_2 Groups							
C2CC=C ⇒ C2C=CC•	1	3.83E7	1.85	2.42	0.97	0.95	0.94
		5.03E7	**1.81**	**2.48**			
C2CC=C ⇒ C2C=CC•	1	5.97E7	1.78	2.30	0.85	0.94	0.97
		4.46E7	**1.81**	**2.24**			
CCC(C)C=C ⇒ CCC•(C)C=C	1	3.58E8	1.56	2.99	1.11	1.00	1.01
		4.82E7	**1.81**	**2.59**			
average (restricted fits)		**4.8E7**	**1.81**	**2.4**			
standard deviation		**2.9E6**		**0.18**			

are divided into two parts; results for linear alkenes are presented first, followed by those for branched and conjugated alkenes. Again, two sets of Arrhenius parameters are reported, the latter one (in bold) being obtained via a restricted fit with a constant n value of 2.28. A closer look at the data reveals the following. (1) The A factors of the restricted fits of all reactions are reasonably close together, and no correlation to the alkene structure is observable. (2) The "activation" energies E of most of the reactions also group together well. However, a few reactions involving branched reactants have clearly lower barriers (e.g., CCC(C)=C). For one reactant, C=C(C)C=C, the barrier is higher than average. The reaction with the highest E value is the least exothermic reaction, but no clear correlation exists between the barrier and heat of reaction. (3) The heats of reaction values for reactants with a conjugated double bond are significantly lower than those of simple alkenes. This increase in exothermicity, however, does not lead to a reduction of the barrier. Essentially, 1,3-dienes react with the same rate constants as do alkenes.

From a selected subset of the data in Table 6, we obtained the following rate rule for H abstraction by H atoms from allyl CH_3 groups

$$k = n_H \cdot 8.1E5\ cm^3/mol\text{-}s \cdot T^{2.28} \cdot \exp(-4.3\ kcal\ mol^{-1}/RT)$$

The quality of the predictions for moderate temperatures is good to fair as can be seen from the two right columns in Table 6. In particular, the reactions of linear alkenes are well represented, but even the worst prediction for C=C(C)C=C is still within a factor of 2.

Because this reaction class produces a resonantly stabilized radical, one would expect the transition state to be aligned in such a way that the breaking bond can overlap with the neighboring double bond. Interestingly, inspection of some of the transition-state structures (e.g., for propene) showed that the B3LYP-optimized transition-state structure deviated significantly from this expected geometry. This leads to the suspicion that the geometries (and possibly frequencies) are not as good as desired and that the CBS-QB3 calculations might need to be replaced with more precise calculation methods, perhaps including multireference ones. Such a study is left for future work. At this point, we therefore can only recommend the rate rules with caution.

To obtain a complete set of rate estimation rules for noncyclic alkenes, we also investigated the abstraction reactions involving secondary and tertiary allylic C−H bonds. The results are presented in Table 7. Even though the test set contains considerably fewer reactions and the reactant structures are not as diverse as those in the primary allyl CH_3 calculations, the consistency in the data is still remarkable. The following generic rate constants lead to a good representation:

allylic CH_2

$$k = n_H \cdot 2.4E7\ cm^3/mol\text{-}s \cdot T^{2.18} \cdot \exp(-3.1\ kcal\ mol^{-1}/RT)$$

allylic CH

$$k = n_H \cdot 4.8E7\ cm^3/mol\text{-}s \cdot T^{1.81} \cdot \exp(-2.4\ kcal\ mol^{-1}/RT)$$

The activation energies of the rate rules, when plotted against the average heat of reaction, form a straight line but with a slope that differs considerably from that seen for alkanes. This is shown in Figure 2 in which the barrier versus heat of reaction data for allylic C−H are plotted as part of the reson.-CH data. The same trend in Evans−Polanyi slopes has also been observed

by Zhang et al.,[42] based on BH&HLYP calculations. Other reaction classes included in the reson.-CH data set are H abstractions from alkynes, allenes, and benzylic C−H from toluene and the three xylene isomers. These results are still preliminary. The slope of 0.4 for the linear relationship can be interpreted in the sense that just a small fraction of the resonance effect that stabilizes the product radicals transfers into the transition state. Taking all information together, this plot nicely confirms the classifications of transition-state-stabilizing factors that were discovered by Hammett and Taft decades ago based on experimental data.

We like to conclude this part of the discussion with two final notes regarding Figure 2. (1) The investigated reactions cover heats of formation ranging from strongly exothermic to slightly endothermic. One can see that the endothermic $\{\Delta_r H,E\}$ data fit well into the overall picture. This means that as long as the same reaction class is considered, there seems to be no need to differentiate these further in terms of exothermicity. (2) Thermodynamic consistency between forward and reverse reaction rate constants demands that the slope of an Evans−Polanyi plot for the reverse direction (m^{rev}) be given by

$$m^{rev} = 1 - m^{for}$$

with m^{for} being the corresponding slope of the forward direction. Therefore, the results presented in this work also serve as a starting point to determine rate estimation rules for H abstraction reactions from H_2 by alkyl radicals. Such an analysis is however outside of the scope of this study and will be left to a separate publication. Instead, we address in the following part a second important issue of automated mechanism generation, the handling of pressure-dependent reactions.

Rate Constants for Pressure-Dependent Reactions. A large fraction of the reactions in gas-phase models are pressure-dependent, which is particularly true for mechanisms used in high-temperature and/or low-pressure applications. The characteristic feature of pressure-dependent reactions is a competition between isomerization and bimolecular product channels on the one hand and (de-) activation collisions on the other hand. The following scheme illustrates this.

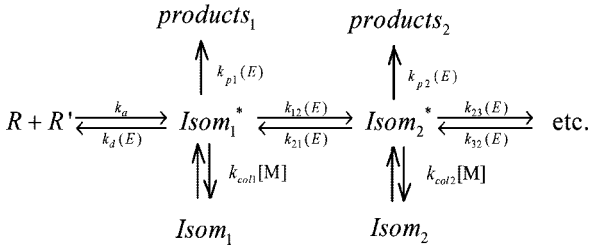

Recombination of R and R′ leads to the formation of an energized adduct called $Isom_1$*. The excess energy originates from the bond formation process. This short-lived intermediate can redissociate to the reactants, form bimolecular products, or isomerize (e.g., to $Isom_2$*). Collisions with the bath gas remove part of the energy of $Isom_1$* and thermalize it to $Isom_1$. All other excited isomers can undergo similar reactions.

SCHEME 1: Reactions of Chemically-Activated Adducts

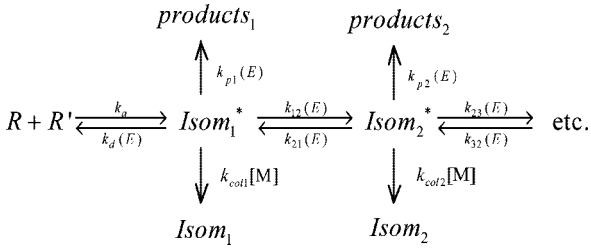

By conceptually dividing this complex system into two time scales, Dean and co-workers[46,78,79] have shown that apparent pressure- and temperature-dependent rate constants for each channel are easily obtained for any multiwell/multichannel system. This division results in (1) fast reactions of the chemically activated species formed in the recombination process, which are dissociations, isomerizations, and irreversible stabilization (Scheme 1)and (2) thermally activated unimolecular reactions of each isomer (Scheme 2). This second group of reactions proceeds on a longer time scale since the thermalized species first need to be reactivated via collisions. The following scheme shows this for $Isom_1$; similar schemes apply for the other isomers. (Note, that the dissociation to the reactants is now irreversible and that $Isom_1$ can now be activated and the corresponding excited complex $Isom_1$* deactivated.)

SCHEME 2: Reactions of Thermalized Adducts

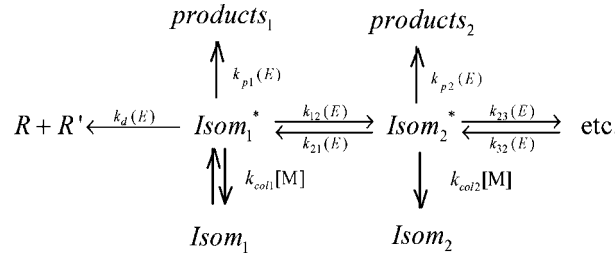

The chemical activation and thermal dissociation steps are analyzed by invoking the steady-state approximation and calculating the apparent rate constants from the energy-resolved steady-state concentrations. By making the choice to use QRRK theory to calculate the density of the state function and $k(E)$ and the modified strong collision assumption[80,81] to calculate collision efficiencies, the solutions (apparent rate constants) can be obtained solely from easily obtainable (or easy to estimate) input parameters. For example, the differential RRK rate constant for channel l, $k_l(E)$, is given by

$$k_l(E) = A_l \frac{\sum_n N(n - q_l)}{\sum_n N(n)} \qquad \text{with } N(x) = \frac{\Gamma(x + s_l)}{\Gamma(x+1)\Gamma(s_l)}$$

Here, A_l is the pre-exponential Arrhenius factor, q_l is the number of energy quanta corresponding to the barrier height E_l, n is the total energy index ($E = n \cdot h\nu$), and the function $N(x)$ yields the number of ways in which x quanta can be placed in s_l oscillators. To allow for q_l to assume noninteger values, factorials are replaced by the Gamma function. More specifics can be found elsewhere;[78] the purpose of this brief discussion is to show that the calculation of $k(E)$ only requires high-pressure rate information (A_l, E_l) and the representative frequency s_l. (In ref 78, the extension to three representative frequencies is discussed, which considerably improves the accuracy of this approach.) The representative frequency(ies) can be obtained from fits to the entropy and heat capacity data,[82] which in turn are obtained from group additivity.[32] Other required input parameters are Lennard-Jones collision parameters, the average amount of energy transferred in collisions, and the molecular weight.

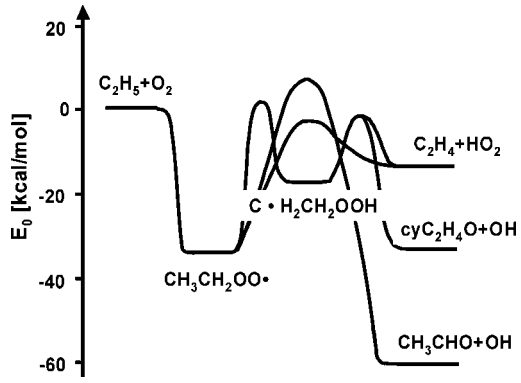

Figure 3. Potential energy surface for the reaction of ethyl radicals with molecular oxygen at the CBS-QB3 level of theory.

The following discussion of the reaction of ethyl radicals with molecular oxygen[83,84] demonstrates that (1) this approach, despite its simplicity, yields very accurate predictions, and (2) pressure variations can have an enormous effect on the total rate constant as well as on product yields. According to the underlying PES (Figure 3), initially formed highly energized ethylperoxy can dissociate to the reactants or several product channels, isomerize to excited hydroperoxyethyl, or lose energy via bath gas collisions to form stabilized ethylperoxy. The excited hydroperoxyethyl radicals will react in a similar manner. This is the chemically activated part of the reaction, and we sometimes refer to the products as "direct" or "prompt" products. Stabilized ethylperoxy and hydroperoxyethyl will undergo, on a longer time scale, unimolecular reactions leading to the same products, which might be called "delayed". In order to fully describe this system, we need to calculate apparent rate constants for 15 reactions (see Figure 4); however, not all of them are important. For example, at low to medium temperatures, only three channels need to be considered to essentially capture the chemistry. These are the formation of ethylperoxy from ethyl + O_2 (reaction 1), the prompt formation of ethylene and HO_2 (reaction 2), and the delayed formation of ethylene and HO_2 from ethylperoxy (reaction 8 in Figure 4).

Figure 5A shows the total rate constant for ethyl + O_2 as a function of pressure for three different temperatures. With a slightly increased total cross section,[83] the QRRK/MSC calculation successfully reproduces the experimentally observed falloff behavior. It is also evident that doubling the temperature causes the falloff curve to shift by about two orders of magnitude to higher pressure. A further increase of the temperature from 600 to 800 K leads to a shift by another order of magnitude. This demonstrates that a rate constant, which might be at the high-pressure limit for certain conditions, can easily be pushed to its falloff region if the temperature increases. Therefore, it is so important to develop kinetic mechanisms that treat pressure-dependent reactions appropriately. Figure 5B emphasizes this point by looking at calculated product distributions at 800 K. At low pressures, the bimolecular product channels dominate, but as the pressure is increased, more of the initially formed adduct is stabilized until stabilization becomes the only important channel.

Finally, we take a closer look at measured and predicted ethylene (relative to ethyl chloride) and hydroperoxy radical yields, which are shown in Figure 6. At low temperatures, most of the initially formed excited ethylperoxy radicals are stabilized, and only small amounts of C_2H_4 and HO_2 are formed. These small yields originate from the prompt dissociation of excited ethylperoxy. As the temperature increases, (in the experiments by Kaiser[85] at around 450 K and in those of Clifford et al.[18] at about 550 K), there is a dramatic increase in the C_2H_4 or HO_2 yield, respectively. The yield increase is caused by thermal decomposition of the ethylperoxy radicals ("delayed"). The QRRK analysis not only captures these experimental observations well but also explains the temperature shift. The photolysis experiments by Kaiser were conducted at 1 atm, and the products were measured by GC after 30 s reaction time, while the HO_2 data from Clifford were obtained after 17 ms and at a substantially lower pressure. Due to the higher pressure and longer residence time, thermal decomposition pathways can contribute in Kaiser's experiments at lower temperatures than those in Clifford's experiment. As a side note, Figure 6 also shows how sensitive these predictions are with respect of the barrier height for the $C_2H_5O_2 \rightleftharpoons C_2H_4 + HO_2$ and that very accurate rate information is needed to obtain accurate predictions.

The ethyl + O_2 reaction is just an example of the large fraction of pressure-dependent reactions that can be found in

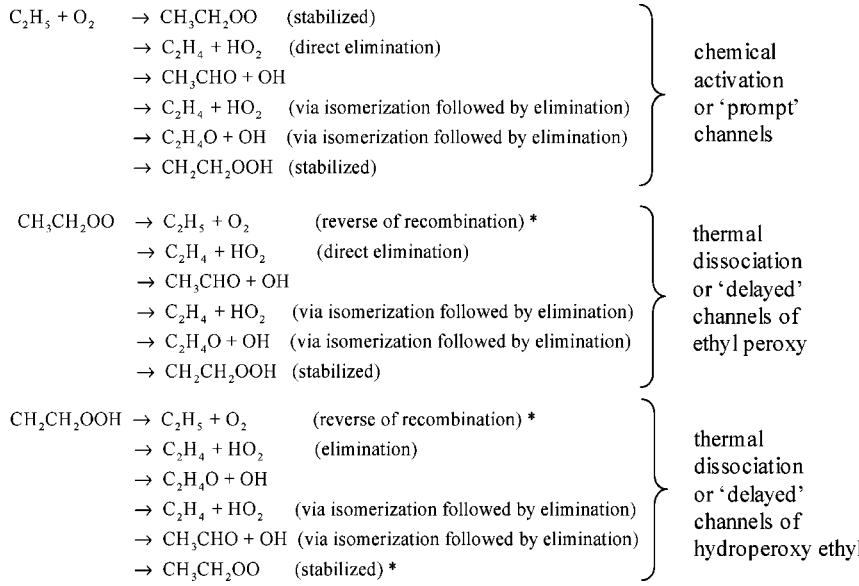

Figure 4. Apparent reaction channels for the ethyl + O_2 reaction. The reactions marked with a * are reverse reactions and not included in the submechanism for this system.

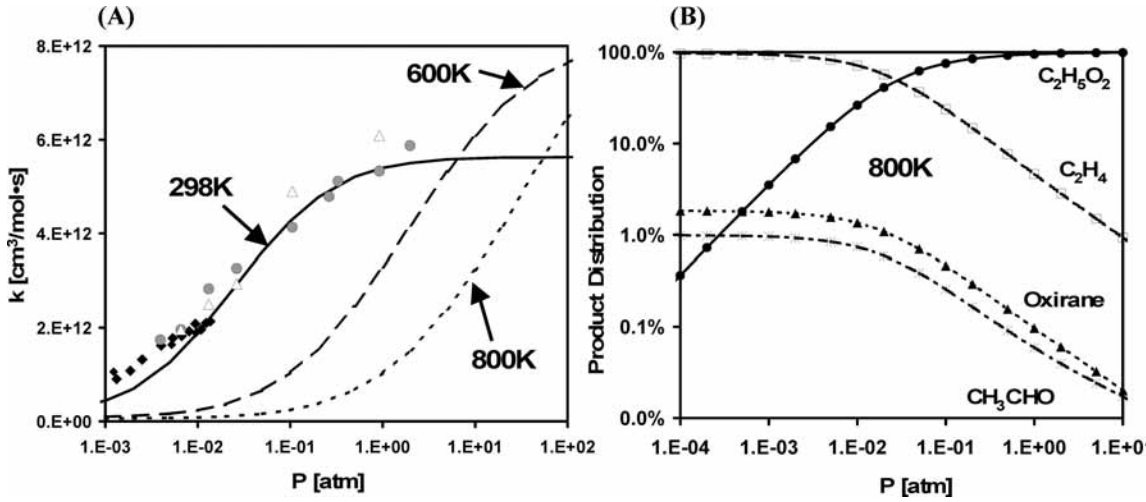

Figure 5. The impact of the total pressure on (A) the total rate constant and (B) the product distribution of the reaction $C_2H_5 + O_2 \Rightarrow$ products. The symbols in (A) represent experimental data from various studies[108−110] to demonstrate the level of agreement of the calculated with the observed total rate constant.

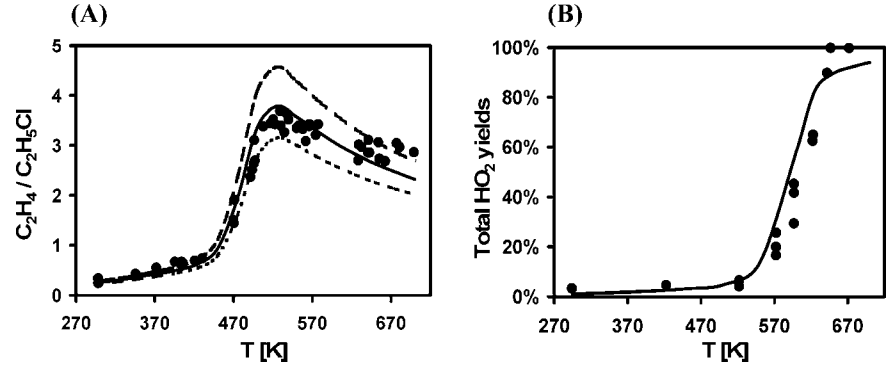

Figure 6. Experimental and predicted C_2H_4 and HO_2 yields, respectively. (Left) Symbols: experimental data from Kaiser (t = 30s, P = 1 atm);[85] solid line: CBS-QB3/QRRK predictions; broken line: barrier increased by 0.2 kcal/mol; dotted line: barrier reduced by 0.2 kcal/mol. (Right) Filled circles: experimental data from Clifford et al. (t = 17 ms, P ~ 1/6 atm);[18] solid line: CBS-QB3/QRRK predictions.

high-temperature gas-phase reaction mechanisms. Given the larger number of reaction types that experience pressure dependence (addition to multiple bonds, radical−radical recombination, bond fission, isomerization, insertion reactions,...), there is an obvious need to be able to identify those reactions and to assign rate constants in an automatic way. The fact that the QRRK/MSC approach yields good predictions and does not require any detailed knowledge of molecular properties of reactants and transition states make it an obvious choice for automated mechanism generation. Matheu[86] implemented this concept into such a code and also added a screening algorithm[87] that removes all of the unimportant channels and thus keeps the representation of pressure-dependent reaction systems for a given application to the minimum number of apparent rate constants. He and co-workers successfully applied this program to the pyrolysis of methane[88] and ethane[89,90] and other systems.[91] However, the full potential of this code can only be developed if rate estimates for all important reaction classes become available. Although some progress has been made in the past few year (see e.g., refs 84, 92−98), more work in this area is needed to cover all important reaction classes.

Conclusions and Suggestions for Future Work

The gas-phase kinetics modeling community is in a transitional phase, moving away from traditional hand-built small mechanisms toward comprehensive computer-generated reaction sets. The implementation and use of automated model generators has its own challenges, especially in the context of generating accurate rate rules, and we discussed in this publication two areas where we think that substantial progress has been made, (1) the development of rate estimation rules for hydrogen abstraction reaction classes while at the same time making sure that reactivity subtleties are not overlooked and (2) the development of an approach to treat pressure dependence that is amenable to computer generation. A common feature of both examples is that the predictions are very sensitive to the barriers, which implies that highly accurate rate rules will be needed to make automatically generated mechanisms successful. A major responsibility of kineticists involved in mechanism development—now relieved from the tedious construction process—will be to provide such high-quality data and to identify inaccurate rate constant information. We will conclude by mentioning a few research avenues that can contribute to meeting this challenge.

Computational chemistry will be an increasingly important source for kinetic and thermodynamic information. Recalling the enormous sensitivity of the rate constant predictions to small changes in barrier heights (Figure 1 and Figure 6), it appears that the definition of chemical accuracy needs to be revised. Fortunately, as the given examples have shown, the relative accuracy of compound methods such as CBS-QB3 is often better than 1 kcal/mol and can possibly be even further improved by applying bond additivity corrections[99] or isodesmic schemes.[100,101] On the other hand, when looking at the reaction sets in, for example, Table 1 or 6, the question arises whether it is possible

to reduce the variations in the *A* factors and barriers even further, so that it would be possible to clearly identify non-next-neighbor effects from "computational noise".

Future work is needed to explore which model chemistry is suitable for a given reaction type. For example, are single reference wave functions still viable for resonantly stabilized reactions? Another area that needs further improvement is the treatment of low-frequency modes. Even though hindered rotors are nowadays routinely separated from harmonic modes, the details of this treatment differ substantially. The methods used to calculate a hindrance potential and the moment of inertia have a profound impact on the entropy contribution[59,102] of these modes. Therefore, further assessment studies involving larger molecules that provide recommendations for this treatment would be desirable. Other issues involve the treatment of low-frequency wagging modes,[8] temperature- or magnitude-dependent frequency scaling factors,[103] and probably mode couplings. Given all of these uncertainties, the observed good agreement between experimental and theoretical data seems fortunate.

Another increasingly important aspect of future modeling will deal with mechanism validation and improvement. Given the huge number of parameters in mechanisms, all of them with their own uncertainties, and simultaneously the errors inherent in the experimental data that are used to validate the mechanisms, the identification and correction of "bad" kinetic data remains a difficult task. Frenklach et al. developed mathematical tools to optimize mechanisms[104] and advertise a collaborative effort to generate new well-defined experimental test sets to validate future mechanisms.[105] Another aspect is to assign realistic uncertainty limits to calculated rate expressions, which can be used by analytic tools as bounds in which such kinetic data may be varied to improve model predictions.

Finally, while rate estimation rules can be applied for many reaction types and classes, there are also special reactions that demand individual studies. One example is the recombination reaction of propargyl radicals, which, despite substantial experimental and theoretical efforts, is still far from being understood.[106] Even the "simple" H_2/O_2 submechanism still requires improvements![107] Therefore, while the applications of gas-phase models rapidly expand toward new and increasingly complex applications—thermal conversion of biomass being currently an area of immense interest—there are still substantial efforts needed to improve our knowledge of small reaction systems. Thus, although the computer might well soon be responsible for mechanism generation, the role of the kineticist is as important as ever, but the job description has been redefined.

Acknowledgment. The authors wish to gratefully acknowledge CPU time allocations on TeraGrid (Grant CHE60032N) and the NREL cluster Lester. The study was partially supported by the Office of Naval Research Grant N00014-05-1-0339 (program manager Dr. Michele L. Anderson).

References and Notes

(1) Poisson, N.; Kanakidou, M.; Crutzen, P. J. *J. Atmos. Chem.* **2000**, *36*, 157.

(2) Ariya, P. A.; Sander, R.; Crutzen, P. J. *J. Geophys. Res.* **2000**, *105*, 17721.

(3) Sjoberg, M.; Dec, J. E. Isolating the Effects of Fuel Chemistry on Combustion Phasing in an HCCI Engine and the Potential of Fuel Stratification for Ignition Control. SAE 2004 World Congress & Exhibition, Detroit, MI, 2004.

(4) Takatori, Y.; Mandokoro, Y.; Akihama, K.; Nakakita, K.; Tsukasaki, Y.; Iguchi, S.; Yeh, L. I.; Dean, A. M. *SAE* **1997**, 982495.

(5) Glaude, P. A.; Melius, C.; Pitz, W. J.; Westbrook, C. K. *Proc. Combust. Inst.* **2002**, *29*, 2469.

(6) Gupta, G. K.; Hecht, E. S.; Zhu, H.; Dean, A. M.; Kee, R. J. *J. Power Sources* **2006**, *156*, 434.

(7) Gupta, G. K.; Dean, A. M.; Hecht, E. S.; Zhu, H.; Kee, R. J. The Influence of Heterogeneous Chemistry and Electrochemistry on Gas-Phase Molecular Weight Growth and Deposit Formation. Solid Oxide Fuel Cells IX, Quebec City, Canada, 2005.

(8) Beste, A.; Buchanan, A. C.; Britt, P. F.; Hathorn, B. C.; Harrison, R. J. *J. Phys. Chem. A* **2007**, *111*, 12118.

(9) Kee, R. J.; Rupley, F. M.; Miller, J. A.; Coltrin, M. E.; Grcar, J. F.; Meeks, E.; Moffat, H. K.; Lutz, A. E.; Dixon-Lewis, G.; Smooke, M. D.; Warnatz, J.; Evans, G. H.; Larson, R. S.; Mitchell, R. E.; Petzold, L. R.; Reynolds, W. C.; Caracotsios, M.; Steward, W. E.; Glarborg, P.; Wang, C.; Adigun, O. *Chemkin Collection*, release 3.6 ed.; Reaction Design, Inc.: San Diego, CA, 2000.

(10) Cantera, Object-Oriented Software for Reacting Flow Simulation. http://www.cantera.org/.

(11) Detailed Chemistry in CFD . http://www.detchem.com/.

(12) Schwer, D. A.; Green, W. H., Jr.; Lu, P. *Combust. Flame* **2003**, *133*, 451.

(13) Ortega, J. M.; Najm, H. N.; Ray, J.; Valorani, M.; Goussis, D. A.; Frenklach, M. *J. Phys.: Conf. Ser. 78* **2007**, 012054.

(14) Turanyi, T. *Comput. Chem.* **1990**, *14*, 253.

(15) Ruscic, B.; Feller, D.; Dixon, D. A.; Peterson, K. A.; Harding, L. B.; Asher, R. L.; Wagner, A. F. *J. Phys. Chem. A* **2001**, *105*, 1.

(16) Berkowitz, J.; Ellison, G. B.; Gutman, D. *J. Phys. Chem.* **1994**, *98*, 2744.

(17) Atkinson, D. B.; Hudgens, J. W. *J. Phys. Chem. A* **1999**, *103*, 4242.

(18) Clifford, E. P.; Farrell, J. T.; DeSain, J. D.; Taatjes, C. A. *J. Phys. Chem. A* **2000**, *104*, 11549.

(19) Chevalier, C.; Pitz, W. J.; Warnatz, J.; Westbrook, C. K.; Melenk, H. *Proc. Combust. Inst.* **1992**, 24.

(20) Broadbelt, L. J.; Stark, S. M.; Klein, M. T. *Chem. Eng. Sci.* **1994**, *49*, 4991.

(21) Broadbelt, L. J.; Stark, S. M.; Klein, M. T. *Ind. Eng. Chem. Res.* **1994**, *33*, 790.

(22) Broadbelt, L. J.; Stark, S. M.; Klein, M. T. *Ind. Eng. Chem. Res.* **1995**, *34*, 2566.

(23) Susnow, R. G.; Dean, A. M.; Green, W. H.; Peczak, P.; Broadbelt, L. J. *J. Phys. Chem. A* **1997**, *101*, 3731.

(24) Green, W. H.; Barton, P. I.; Bhattacharjee, B.; Matheu, D. M.; Schwer, D. A.; Song, J.; Sumathi, R.; Carstensen, H. H.; Dean, A. M.; Grenda, J. M. *Ind. Eng. Chem. Res.* **2001**, *40*, 5362.

(25) Tomlin, A. S.; Turanyi, T.; Pilling, M. J. Mathematical Tools for the Construction, Investigation and Reduction of Combustion Mechanisms. In *Low-Temperature Combustion and Autoignition*; Pilling, M. J., Ed.; Elsevier: Amsterdam, The Netherlands, 1997.

(26) Warth, V.; Stef, N.; Glaude, P. A.; Battin-Leclerc, F.; Scacchi, G.; Come, G. M. *Combust. Flame* **1998**, *114*, 81.

(27) Bournez, O.; Come, G.-M.; Conraud, V.; Kirchner, H.; Ibanescu, L. A Rule-Based Approach for Automated Generation of Kinetic Chemical Mechanisms. In *Rewriting Techniques and Applications*; Springer: Berlin/Heidelberg, Germany, 2003; p 152.

(28) Bounaceur, R.; Warth, V.; Marquaire, P.-M.; Scacchi, G.; Domine, F.; Dessort, D.; Pradier, B.; Brevart, O. *J. Anal. Appl. Pyrolysis* **2002**, *64*, 103.

(29) Warth, V.; Battin-Leclerc, F.; Fournet, R.; Glaude, P. A.; Come, G. M.; Scacchi, G. *Comput. Chem.* **2000**, *24*, 541.

(30) Ratkiewicz, A.; Truong, T. N. *Int. J. Quantum Chem.* **2006**, *106*, 244.

(31) Benson, S. W. *Thermochemical Kinetics*, 2 ed.; John Wiley & Sons: New York, 1976.

(32) Ritter, E. R.; Bozzelli, J. W. *Int. J. Chem. Kinet.* **1991**, *23*, 767.

(33) Lay, T. H.; Bozzelli, J. W.; Dean, A. M.; Ritter, E. R. *J. Phys. Chem.* **1995**, *99*, 14514.

(34) Sumathi, R.; Green, W. H., Jr. *Theor. Chem. Acc.* **2002**, *108*, 187.

(35) Hammett, L. P. *J. Am. Chem. Soc.* **1937**, *59*, 96.

(36) Taft, R. W., Jr. *J. Am. Chem. Soc.* **1952**, *74*, 2729.

(37) Evans, M. G.; Polanyi, M. *Trans. Faraday Soc.* **1938**, *34*, 11.

(38) Evans, M. G.; Polanyi, M. *Proc. R. Soc. London, Ser. A* **1936**, *154*, 133.

(39) Sumathi, R.; Carstensen, H.-H.; Green, W. H., Jr. *J. Phys. Chem. A* **2001**, *105*, 6910.

(40) Sumathi, R.; Carstensen, H.-H.; Green, W. H., Jr. *J. Phys. Chem. A* **2001**, *105*, 8969.

(41) Saeys, M.; Reyniers, M.-F.; Speybroeck, V. V.; Waroquier, M.; Marin, G. B. *ChemPhysChem* **2006**, *7*, 188.

(42) Zhang, S.; Truong, T. N. *J. Phys. Chem. A* **2003**, *107*, 1138.

(43) Mokrushin, V.; Bedanov, V.; Tsang, W.; Zachariah, M.; Knyazev, V. *ChemRate*; 1.19 ed.; NIST: Gaithersburg, MD, 1996−2002.

(44) Barker, J. R. *Int. J. Chem. Kinet.* **2001**, *33*, 232.

(45) Klippenstein, S. J.; Wagner, A. F.; Dunbar, R. C.; Wardlaw, D. M.; Robertson, S. H.; Miller, J. A. *VARIFLEX*, 1.07 ed.; 1999.

(46) Dean, A. M. *J. Phys. Chem.* **1985**, *89*, 4600.
(47) Baboul, A. G.; Curtiss, L. A.; Redfern, P. C.; Raghavachari, K. *J. Chem. Phys.* **1999**, *110*, 7650.
(48) Montgomery, J. J. A.; Frisch, M. J.; Ochterski, J. W.; Petersson, G. A. *J. Chem. Phys.* **2000**, *112*, 6532.
(49) Ochterski, J. W.; Petersson, G. A.; Montgomery, J. A., Jr. *J. Chem. Phys.* **1996**, *104*, 2598.
(50) Martin, J. M. L.; de Oliveira, G. *J. Chem. Phys.* **1999**, *111*, 1843.
(51) Helgaker, T.; Ruden, T. A.; Jorgensen, P.; Olsen, J.; Klopper, W. *J. Phys. Org. Chem.* **2004**, *17*, 913.
(52) Vandeputte, A. G.; Sabbe, M. K.; Reyniers, M.-F.; Van Speybroeck, V.; Waroquier, M.; Marin, G. B. *J. Phys. Chem. A* **2007**, *111*, 11771.
(53) Adamo, C.; Barone, V. *J. Chem. Phys.* **1998**, *108*, 664.
(54) Boese, A. D.; Martin, J. M. L. *J. Chem. Phys.* **2004**, *121*, 3405.
(55) Carstensen, H.-H.; Dean, A. M.; Deutschmann, O. *Proc. Combust. Inst.* **2007**, *31*, 149.
(56) Frisch, M. J.; Trucks, G. W.; Schlegel, H. B.; Scusera, G. E.; Robb, M. A; Cheeseman, J. R.; Zakrzewski, V. G.; Montgomery, J. A.; Stratmann, R. E., Jr.; Burant, J. C.; Dapprich, S.; Millam, J. M.; Daniels, A. D.; Kudin, K. N.; Strain, M. C.; Farkas, O.; Tomasi, J.; Barone, V.; Cossi, M.; Cammi, R.; Mennucci, B.; Pomelli, C.; Adamo, C.; Clifford, S.; Ochterski, J.; Petersson, G. A.; Ayala, P. Y.; Cui, Q.; Morokuma, K.; Malick, D. K.; Rabuck, A. D.; Raghavachari, K.; Foresman, J. B.; Cioslowski, J.; Ortiz, J. V.; Baboul, A. G.; Stefanov, B. B.; Liu, G.; Liashenko, A.; Piskorz, P.; Komaromi, I.; Gomperts, R.; Martin, R. L.; Fox, D. J.; Keith, T.; Al-Laham, M. A.; Peng, C. Y.; Nanayakkara, A.; Gonzalez, C.; Challacombe, M.; Gill, P. M. W.; Johnson, B.; Chen, W.; Wong, M. W.; Andres, J. L.; Gonzalez, C.; Head-Gordon, M.; Replogle, E. S.; Pople, J. A. *Gaussian 98*, revision A.11; Gaussian, Inc.: Pittsburgh, PA, 1998.
(57) Frisch, M. J.; Trucks, G. W.; Schlegel, H. B.; Scuseria, G. E.; Robb, M. A.; Cheeseman, J. R.; Montgomery, J. A., Jr.; Vreven, T.; Kudin, K. N.; Burant, J. C.; Millam, J. M.; Iyengar, S. S.; Tomasi, J.; Barone, V.; Mennucci, B.; Cossi, M.; Scalmani, G.; Rega, N.; Petersson, G. A.; Nakatsuji, H.; Hada, M.; Ehara, M.; Toyota, K.; Fukuda, R.; Hasegawa, J.; Ishida, M.; Nakajima, T.; Honda, Y.; Kitao, O.; Nakai, H.; Klene, M.; Li, X.; Knox, J. E.; Hratchian, H. P.; Cross, J. B.; Bakken, V.; Adamo, C.; Jaramillo, J.; Gomperts, R.; Stratmann, R. E.; Yazyev, O.; Austin, A. J.; Cammi, R.; Pomelli, C.; Ochterski, J. W.; Ayala, P. Y.; Morokuma, K.; Voth, G. A.; Salvador, P.; Dannenberg, J. J.; Zakrzewski, V. G.; Dapprich, S.; Daniels, A. D.; Strain, M. C.; Farkas, O.; Malick, D. K.; Rabuck, A. D.; Raghavachari, K.; Foresman, J. B.; Ortiz, J. V.; Cui, Q.; Baboul, A. G.; Clifford, S.; Cioslowski, J.; Stefanov, B. B.; Liu, G.; Liashenko, A.; Piskorz, P.; Komaromi, I.; Martin, R. L.; Fox, D. J.; Keith, T.; Al-Laham, M. A.; Peng, C. Y.; Nanayakkara, A.; Challacombe, M.; Gill, P. M. W.; Johnson, B.; Chen, W.; Wong, M. W.; Gonzalez, C.; Pople, J. A. *Gaussian 03*, revision C.2; Gaussian, Inc.: Pittsburgh, PA, 2003.
(58) Becke, A. D. *J. Chem. Phys.* **1993**, *98*, 5648.
(59) East, A. L. L.; Radom, L. *J. Chem. Phys.* **1997**, *106*, 6655.
(60) Kilpatrick, J. E.; Pitzer, K. S. *J. Chem. Phys.* **1949**, *17*, 1064.
(61) Eckart, C. *Phys. Rev.* **1930**, *35*, 1303.
(62) Wigner, E. *Z. Phys. Chem.* **1932**, *B 19*, 203.
(63) Skodje, R. T.; Truhlar, D. G.; Garrett, B. C. *J. Phys. Chem.* **1981**, *85*, 3019.
(64) Truong, T. N.; Duncan, W. T.; Tirtowidjojo, M. *Phys. Chem. Chem. Phys.* **1999**, *1*, 1061.
(65) Sutherland, J. W.; Su, M.-C.; Michael, J. V. *Int. J. Chem. Kinet.* **2001**, *33*, 669.
(66) Konkoli, Z.; Kraka, E.; Cremer, D. *J. Phys. Chem. A* **1997**, *101*, 1742.
(67) Bryukov, M. G.; Slagle, I. R.; Knyazev, V. D. *J. Phys. Chem. A* **2001**, *105*, 3107.
(68) Kerkeni, B.; Clary, D. C. *Phys. Chem. Chem. Phys.* **2006**, *8*, 917.
(69) Huarte-Larranaga, F.; Manthe, U. *J. Chem. Phys.* **2002**, *116*, 2863.
(70) Pu, J.; Truhlar, D. G. *J. Chem. Phys.* **2002**, *117*, 1479.
(71) Yu, H.-G.; Nyman, G. *J. Chem. Phys.* **1999**, *111*, 3508.
(72) Jordan, M. J. T.; Gilbert, R. G. *J. Chem. Phys.* **1995**, *102*, 5669.
(73) Baulch, D. L.; Bowman, C. T.; Cobos, C. J.; Cox, R. A.; Just, T.; Kerr, J. A.; Pilling, M. J.; Troe, J.; Tsang, W.; Walker, R. W.; Warnatz, J. *J. Phys. Chem. Ref. Data* **2005**, *34*, 757.
(74) Tsang, W.; Hampson, R. F. *J. Phys. Chem. Ref. Data* **1986**, *15*, 1087.
(75) Dean, A. M.; Bozzelli, J. W. Combustion Chemistry of Nitrogen. In *Gas-Phase Combustion Chemistry*; Gardiner, W. C., Ed.; Springer: New York, 2000; p 125.
(76) McMillen, D. F.; Golden, D. M. *Annu. Rev. Phys. Chem.* **1982**, *33*, 493.
(77) Tian, Z.; Fattahi, A.; Lis, L.; Kass, S. R. *J. Am. Chem. Soc.* **2006**, *128*, 17087.
(78) Chang, A. Y.; Bozzelli, J. W.; Dean, A. M. *Z. Phys. Chem.* **2000**, *214*, 1533.
(79) Dean, A. M.; Bozzelli, J. W.; Ritter, E. R. *Combust. Sci. Technol.* **1991**, *80*, 63.
(80) Troe, J. *J. Phys. Chem.* **1979**, *83*, 114.
(81) Gilbert, R. G.; Luther, K.; Troe, J. *Ber. Bunsen-Ges. Phys. Chem.* **1983**, *87*, 169.
(82) Bozzelli, J. W.; Chang, A. Y.; Dean, A. M. *Int. J. Chem. Kinet.* **1997**, *29*, 161.
(83) Carstensen, H.-H.; Naik, C. V.; Dean, A. M. *J. Phys. Chem. A A* **2005**, *109*, 2264.
(84) Carstensen, H.-H.; Dean, A. M. The Kinetics of Pressure-Dependent Reactions. In *Comprehensive Chemical Kinetics*; Elsevier: Amsterdam, The Netherlands, 2007; p 105.
(85) Kaiser, E. W. *J. Phys. Chem. A* **2002**, *106*, 1256.
(86) Matheu, D. M. Integrated Pressure-Dependence in Automated Mechanism Generation: A New Tool for Building Gas-Phase Kinetic Models. Ph.D. Thesis, Massachusetts Institute of Technology, 2003.
(87) Matheu, D. M.; Lada, T. A., II; Green, W. H.; Dean, A. M.; Grenda, J. M. *Comput. Phys. Commun.* **2001**, *138*, 237.
(88) Matheu, D. M.; Dean, A. M.; Grenda, J. M.; Green, W. H., Jr. *J. Phys. Chem. A* **2003**, *107*, 8552.
(89) Matheu, D. M.; Grenda, J. M. *J. Phys. Chem. A* **2005**, *109*, 5332.
(90) Matheu, D. M.; Grenda, J. M. *J. Phys. Chem. A* **2005**, *109*, 5343.
(91) Matheu, D. M.; Green, W. H., Jr.; Grenda, J. M. *Int. J. Chem. Kinet.* **2003**, *35*, 95.
(92) Harding, L. B.; Georgievskii, Y.; Klippenstein, S. J. *J. Phys. Chem. A* **2005**, *109*, 4646.
(93) Klippenstein, S. J.; Georgievskii, Y.; Harding, L. B. *Phys. Chem. Chem. Phys.* **2006**, *8*, 1133.
(94) Georgievskii, Y.; Miller, J. A.; Klippenstein, S. J. *Phys. Chem. Chem. Phys.* **2007**, *9*, 4259.
(95) Harding, L. B.; Klippenstein, S. J.; Georgievskii, Y. *J. Phys. Chem. A* **2007**, *111*, 3789.
(96) da Silva, G.; Bozzelli, J. W. *JJ. Phys. Chem. A* **2008**, *112*, 3566.
(97) Sabbe, M. K.; Reyniers, M.-F.; Speybroeck, V. V.; Waroquier, M.; Marin, G. B. *ChemPhysChem* **2008**, *9*, 124.
(98) Ogura, T.; Miyoshi, A.; Koshi, M. *Phys. Chem. Chem. Phys.* **2007**, *9*, 5133.
(99) Petersson, G. A.; Malick, D. K.; Wilson, W. G.; Ochterski, J. W.; Montgomery, J. A., Jr.; Frisch, M. J. *J. Chem. Phys.* **1998**, *109*, 10570.
(100) Fishtik, I.; Datta, R.; Liebman, J. F. *J. Phys. Chem. A* **2003**, *107*, 695.
(101) Knyazev, V. D. *J. Phys. Chem. A* **2003**, *107*, 11082.
(102) Wong, B. M.; Raman, S. *J. Comput. Chem.* **2007**, *28*, 759.
(103) Irikura, K. K.; Johnston, R. D., III; Kacker, R. N. *J. Phys. Chem. A* **2005**, *109*, 8430.
(104) Frenklach, M.; Wang, H.; Rabinowitz, M. J. *Prog. Energy Combust. Sci.* **1992**, *18*, 47.
(105) Frenklach, M. *Proc. Combust. Inst.* **2007**, *31*, 125.
(106) Tang, W.; Tranter, R. S.; Brezinsky, K. *J. Phys. Chem. A* **2006**, *110*, 2165.
(107) Konnov, A. A. *Combust. Flame* **2008**, *152*, 507.
(108) Slagle, I. R.; Feng, Q.; Gutman, D. *J. Phys. Chem.* **1984**, *88*, 3648.
(109) Plumb, I. C.; Ryan, K. R. *Int. J. Chem. Kinet.* **1981**, *13*, 1011.
(110) Kaiser, E. W.; Wallington, T. J.; Andino, J. M. *Chem. Phys. Lett.* **1990**, *168*, 309.

JP804939V